Millimeter wave radiation-induced magnetoresistance oscillations in the high quality GaAs/AlGaAs 2D electron system under bichromatic excitation

B. Gunawardana, H.-C. Liu, R. L. Samaraweera, M. S. Heimbeck, H. O. Everitt, J. Iñarrea, C. Reichl, W. Wegscheider, and R. G. Mani

Phys. Rev. B **95**, 195304 — Published 3 May 2017

DOI: 10.1103/PhysRevB.95.195304

Millimeter wave radiation-induced magnetoresistance oscillations in the high quality GaAs/AlGaAs 2D electron system under bichromatic excitation

B. Gunawardana,[1] H-C. Liu,[1] R. L. Samaraweera,[1] M. S. Heimbeck,[2] H. O. Everitt,[2,3] J. Iñarrea,[4] C. Reichl,[5] W. Wegscheider,[5] and R. G. Mani[1,*]

[1] *Department of Physics and Astronomy, Georgia State University, Atlanta, Georgia 30303*
[2] *Army Aviation & Missile RD&E Center, Redstone Arsenal, Huntsville, Alabama 35898*
[3] *Dept. of Physics, Duke University, Surham, NC 27708*
[4 1] *Escuela Politécnica Superior,Universidad Carlos III,Leganes,Madrid,28911 ,Spain*
[2] *Unidad Asociada al Instituto de Ciencia de Materiales, CSIC, Cantoblanco,Madrid,28049,Spain.*
[5] *Laboratorium für Festkörperphysik, ETH Zürich, CH-8093 Zürich, Switzerland*

(Dated: February 21, 2017)

Millimeter wave radiation-induced magneto-resistance oscillations are examined in the GaAs/AlGaAs 2D electron system under bichromatic excitation in order to study the evolution of the oscillatory diagonal magnetoresistance, R_{xx} as the millimeter wave intensity is changed systematically for various frequency combinations. The results indicate that at low magnetic fields, the lower frequency millimeter wave excitation sets the observed R_{xx} response, as the higher frequency millimeter wave component determines the R_{xx} response at higher magnetic fields. The observations are qualitatively explained in terms of the order of the involved transitions. The results are also modeled using the radiation-driven electron orbit theory.

I. INTRODUCTION

Transport at large filling factors have been a topic of interest,[1–65] especially the microwave,- millimeter wave,- and terahertz,- radiation-induced zero-resistance states,[1,2] and the associated 1/4-cycle phase shifted radiation-induced magnetoresistance oscillations,[1,3,4,8,9,12,15,17,19,21,25] which refers to the B^{-1}-periodic oscillatory variation in the magnetoresistance observed under photoexcitation in the 2D electron system under the influence of a transverse magnetic field, B. Such oscillations exhibit a non-linear variation in the oscillatory amplitude with radiation power,[15,25,36] sensitivity in the oscillatory amplitude to the orientation of the linearly polarized radiation with respect to the device,[19,25–28,35] etc. Many theoretical explanations have been proposed to help understand associated phenomena,[36–43,45–51,53–64] including, for example, mechanisms based on (a) the scattering of electrons by phonons and impurities between Landau levels,[37,40,42,43] (b) the periodic motion of electron orbit centers under photoexcitation,[38,48], (c) the inelastic model,[45] and (d) the re-collision of cyclotron electrons from scattering centers.[63]

Previous work[6,8,47] has suggested a relationship between the monochromatic and the bichromatic photo induced oscillatory response which can best be described as an average superposition of two monochromatic photo responses.[6,47] In order to obtain a better understanding of this radiation-induced transport under bichromatic excitation, millimeter wave radiation-induced magnetoresistance oscillations are examined here under bichromatic excitation with frequencies f_1 AND f_2 showing ratios f_1/f_2 ranging from $1.84 \leq f_1/f_2 \leq 3.4$, such that the frequency ratios span both the situations where the two frequencies, and hence the associated oscillations, are close together and also when they are further apart on the B-scale. In addition, the radiation power is changed systematically to study the continuous evolution of the lineshape in going from the monochromatic to the bichromatic photoexcitation situation. From the results, we identify a novel trend observed in the crossover from the monochromatic- to the bichromatic- response in R_{xx}, which is attributed here to the order of the involved transitions and simulated with the radiation-driven electron orbit theory.

II. EXPERIMENT AND RESULTS

Measurements were carried out on GaAs/AlGaAs 2D heterostructure samples with an electron density of $3.3 \times 10^{11} cm^{-2}$ and mobility $\mu = 15 \times 10^6 cm^2/Vs$ at $T = 1.7K$. Two sources served to produce millimeter waves at two different frequencies, and bichromatic photoexcitation of the specimen was realized by combining the output of these two sources with a waveguide coupler. A long cylindrical wave guide served to transport the bichromatic millimeter wave radiation to the sample. Here, millimeter waves at both frequencies were co-linearly polarized.

In such experiments, the sample was first illuminated with monochromatic millimeter waves at frequency f_1, with the other millimeter wave source at f_2 switched off, to obtain the R_{xx} vs. B response at f_1. Then, the source at f_1 was switched off, and the source at f_2 was switched on, to obtain the R_{xx} vs. B response at f_2. Finally, the sources at both f_1 AND f_2 were switched on for the bichromatic photo-excitation experiment. The absolute source-power at each f could be set as desired using either variable attenuators or by setting the power at the source. Traces of R_{xx} vs. B obtained, for example, at fre-

quency combinations of $f_1 = 90.6$GHz and $f_2 = 41.0$GHz and $f_1 = 90.6$GHz and $f_2 = 48.7$GHz are shown in Fig. 1(a) and Fig. 1(b), respectively. Here, the source power at $f_1 = 90.6$ GHz was 4 mW. The source powers at f_2 are indicated in the figures. The characteristic fields, B_{f1} and B_{f2}, for frequencies f_1 and f_2, respectively, have been marked in the figures. Here, $B_f = 2\pi f m^*/e$. These frequency ratios highlight the situations where the two frequencies, the characteristic fields, and hence the associated oscillations, are close together on the B-scale.

The reason for setting the lower frequency at 41.0 GHz and 48.7 GHz, when the higher frequency is fixed at 90.6GHz, can be understood by examining Fig. 1. When the specimen is photoexcited by monochromatic millimeter wave radiation at 41.0 GHz and 90.6 GHz, there is coincidence between two peaks in R_{xx} at 90.6 GHz with a valley and a peak in the monochromatic R_{xx} response at 41.0 GHz at magnetic fields $B \approx 0.075$ T and $B \approx 0.055$ T (labeled as (1) and (0) in Fig. 1(a), respectively). When the 2DES is photo-excited separately by millimeter waves at 48.7 GHz and 90.6 GHz, two magnetoresistance valleys in R_{xx} observed at 90.6 GHz coincide with a peak and valley observed at 48.7 GHz, at magnetic fields $B \approx 0.062$ T and $B \approx 0.09$ T, labeled as (0) and (1), respectively, see Fig. 1(b), in the monochromatic R_{xx} millimeter wave response at those f. Thus, the millimeter wave frequencies in the bichromatic experiment have been chosen to achieve coincidence between selected extrema of the two components in order to examine the influence of one extrema upon the other when, say, the millimeter wave intensity of the low frequency component f_2 is varied.

A close examination of the bichromatic response at such frequency ratios have suggested that at "low-B,", i.e., $B < B_{f2}$, the low frequency component can overwhelm the high frequency component, as the source millimeter wave power at the low frequency is progressively increased. Note that the maximum source power for the two frequency components is the same here. For example, by comparing the R_{xx} response in Fig. 1(a) for monochromatic excitation at 90.6 GHz and 41.0 GHz, with the bichromatic response trace at 90.6 GHz;41.0 $GHz, 4mW$, it can be observed that the the bichromatic millimeter wave induced magnetoresistance oscillations at magnetic fields ≤ 0.125 T follows the monochromatic low frequency response of 41 GHz. On the other hand, at "higher-B," i.e., $B_{f2} < B < B_{f1}$, around the region labeled by (2) in Fig. 1, the high frequency component continues to set the bichromatic response, even as the source millimeter wave power at the low frequency is progressively increased. For example, at $0.125 \leq B \leq 0.2$ T, the bichromatic oscillatory response of R_{xx} remains close to the monochromatic high frequency response in both Fig. 1(a) and Fig. 1(b). At even higher B, i.e., $B > B_{f1}$ in the regime of SdH oscillations, around the region labeled by (3) in Fig. 1, the bichromatic response tends to follow the lower monochromatic R_{xx} response in both Fig. 1(a) and Fig. 1(b).

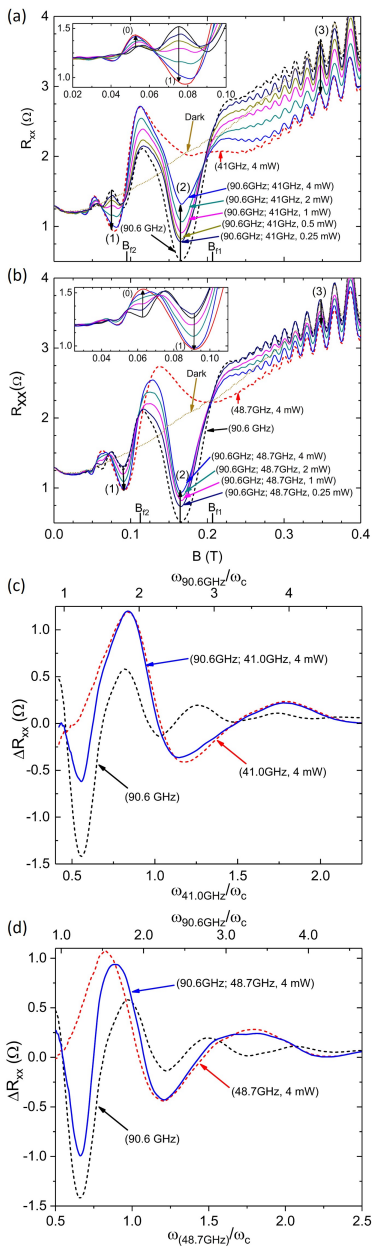

FIG. 1. The diagonal resistance, R_{xx}, exhibits millimeter wave induced magneto-resistance oscillations under bichromatic excitation for frequency pairs: (a) 90.6 GHz and 41.0 GHz and (b) 90.6 GHz and 48.7 GHz, for millimeter wave power $P = 4,\ 2,\ 1,\ 0.5$ and 0.25 mW at the lower frequency, f_2, and constant source power of 4 mW at the higher frequency, f_1. In these figures, (0), (1), (2) and (3) indicate four B-values of special interest for the bichromatic R_{xx} oscillatory response. The inset of both (a) and (b) show an expanded view of the R_{xx} oscillatory response around region (0) and (1). The characteristic fields, B_{f1} and B_{f2}, for f_1 and f_2, respectively, have been marked in the figures. Here, $B_f = 2\pi f m^*/e$. Panels (c) and (d) show selected curves plotted vs. a normalized inverse magnetic field scale with respect to the low (bottom) and high (top) frequency components. Note that the bichromatic signal follows the low frequency component for $\omega_{41.0GHz}/\omega_c > 1$ in (c) and $\omega_{48.7Ghz}/\omega_c > 1$ in (d).

The predominance of the low frequency component at low B or high B^{-1} can also be seen in Fig. 1(c) and 1(d) which show the oscillatory signal ΔR_{xx} vs ω_{f2}/ω_c on the bottom abscissa and ω_{f1}/ω_c on the top abscissa. Here the magnetic field dependent cyclotron frequency $\omega_c(B) = eB/m^*$, where e is the charge of an electron and m^* is the cyclotron effective mass of electron. Further, $\omega_f = 2\pi f$. In both Fig. 1(c) and Fig. 1(d), it is clear that for $\omega_{f2}/\omega_c \geq 1$, the bichromatic signal follows the monochromatic low frequency signal at f_2.

We have also examined the bichromatic response at frequency ratios that produce magnetoresistance oscillations that are further apart on the B-scale in the monochromatic excitation condition, see Fig. 2. Here, the low frequency component has been set at $f_2 = 58\ GHz$, and the high frequency (f_1) component was set sequentially at $141, 156.5, 161$ and $174\ GHz$. The results of such measurements, shown in Fig. 2, indicate once again that the monochromatic low (f_2) frequency R_{xx} response sets bichromatic R_{xx} response at low magnetic fields, i.e., $B < B_{f2}$, as the monochromatic high (f_1) frequency R_{xx} response mostly determines the bichromatic R_{xx} response at the higher magnetic fields, i.e., $B_{f2} < B < B_{f1}$, corresponding to the higher frequency in the bichromatic experiment. These results show that the bichromatic response does not simply depend on the frequency ratio f_1/f_2 or the monochromatic oscillatory responses, but also it seems to depend upon the magnetic field strength as well. Some other noteworthy features in Fig. 2 are indications of the $\sim 2\omega_c$ cyclotron resonance resistance spike[14] observed for the condition $hf \sim 2\hbar\omega_c$ in both the high frequency monochromatic- and the bichromatic- excitation measurements. Such features are observable in the vicinity of the arrowhead for the high frequency monochromatic trace label in Fig. 2. Thus, the $\sim 2\omega_c$ cyclotron resonance resistance spike seems also obervable in this bichromatic experiment. Once again, the predominance of the low frequency component at low B or high B^{-1} can also be seen in Fig. 2(b) and 2(c) which show the oscillatory signal ΔR_{xx} vs ω_{f2}/ω_c on the bottom abscissa and ω_{f1}/ω_c on the top abscissa. In both Fig. 2(b) and Fig. 2(c), it is clear that for $\omega_{f2}/\omega_c \geq 1$, the bichromatic signal follows the monochromatic low frequency signal at f_2.

Published studies of millimeter wave induced magnetoresistance oscillations for monochromatic excitation have shown a non linear relationship between power, P, and the extremal R_{xx}[15,25,36] consistent with both the radiation-driven electron orbit model[38] and the displacement model[37,40,42]. Thus, in the bichromatic experiment corresponding to Fig. 1, i.e., with $f_1 = 90.6$ GHz and $f_2 = 41.0$GHz or $f_2 = 48.7$ GHz, we have examined the power, P, evolution of R_{xx}, when the source power at the low frequency, f_2 is progressively increased from $0.25\ mW$ up to $4.0\ mW$. The results of such measurements at the B labeled (1), (2), and (3) in Fig. 1 are shown in Fig. 3. Fig. 3 shows that even in the bichromatic experiment, there is a non-linear relationship be-

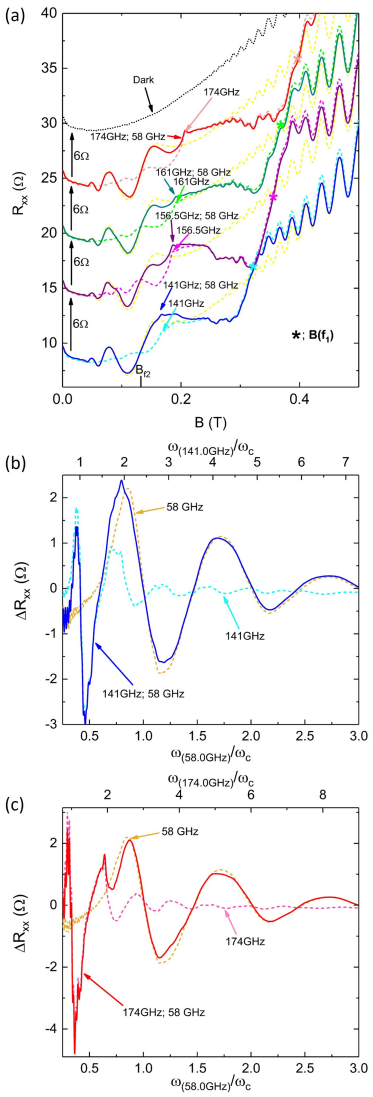

FIG. 2. The diagonal resistance, R_{xx}, exhibits millimeter wave induced magneto-resistance oscillations under bichromatic excitation with the low frequency, f_2, component fixed at 58 GHz as the high frequency, f_1, component takes on the values 141, 156.5, 161, and 174 GHz. Here, the traces have been shifted along the ordinate by 6Ω for the sake of presentation. The characteristic fields, B_{f1} and B_{f2}, for f_1 and f_2, respectively, have been marked in the figure. Here, $B_f = 2\pi f m^*/e$. The solid yellow lines show the monochromatic response of R_{xx} at $f_2 = 58\ GHz$. The nominal source power for f_1 is 10 to 20 mW and f_2 is $\approx$ 10 mW. The plot also shows indications of the $\sim 2\omega_c$ cyclotron resonance resistance spike in both the high frequency monochromatic and the bichromatic excitation measurements near the arrowhead associated with the high frequency monochromatic trace label. Panels (b) and (c) show selected curves plotted vs. a normalized inverse magnetic field scale with respect to the low (bottom) and high (top) frequency components. Note that the bichromatic signal follows the low frequency component for $\omega_{58.0GHz}/\omega_c > 1$ in (b) and $\omega_{58.0Ghz}/\omega_c > 1$ in (c)
.

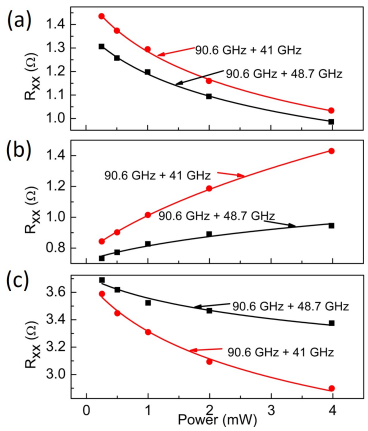

FIG. 3. The variation in the diagonal resistance, R_{xx}, with the change in the millimeter wave power of the low frequency component under bichromatic photo-excitation conditions for (a) region (1), (b) region (2), and (c) region (3), indicated in Fig. 1.

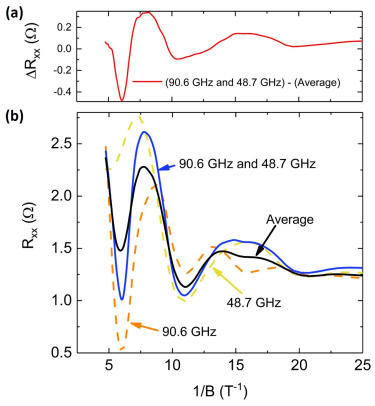

FIG. 4. (a) The difference between the bichromatic (blue trace, panel (b), below) and average responses (black trace, panel (b), below). (b) R_{xx} vs. B^{-1} for monochromatic excitation at 90.6 GHz (dashed brown), 48.7 GHz (dashed lime green), bichromatic excitation at 90.6 GHz and 48.7 GHz,(blue) and the numerical arithmetic average of the monochromatic signals at 90.6 GHz and 48.7 GHz(black). The monochromatic responses were obtained with source excitation at $4mW$, the bichromatic excitation response was obtained with both sources at $4mW$.

tween P and the R_{xx}, as in the extremal P response in the monochromatic experiment.[15,25,36].

Previous studies of the bichromatic microwave induced magnetoresistance oscillations have suggested that the bichromatic response may be the average of the two constituent monochromatic oscillatory responses.[6,47] Thus, for $f_1 = 90.6\ GHz$ and $f_2 = 48.7\ GHz$, with the source power for both components at $4mW$, we have evaluated the average response $R_{xx}(Average) = [R_{xx}(90.6\ GHz) + R_{xx}(48.7\ GHz)]/2$ and plotted the results vs. $1/B$ in Fig. 4(b). Fig. 4(b) shows the evaluated $R_{xx}(Average)$ along with the experimental monochromatic response at $f_1 = 90.6\ GHz$, $f_2 = 48.7\ GHz$ and the bichromatic oscillatory response at $f_1\ AND\ f_2$ as a function of the inverse magnetic field, $1/B$. The results suggest a substantial difference between the $R_{xx}(Average)$ and the bichromatic response over the entire B^{-1} scale. The difference is plotted in Fig. 4(a). The observed difference can be attributed to the afore-mentioned observation that at "low-B", i.e., $B < B_{f2}$, the bichromatic response follows the low frequency response, and it shifts towards the high frequency response at "higher-B", i.e., $B_{f2} < B < B_{f1}$.

III. DISCUSSION

The bichromatic millimeter wave response of the diagonal resistance, R_{xx} follows the low frequency monochromatic response at low magnetic fields, and it deviates towards high frequency monochromatic millimeter wave response as the magnetic field strength increases above B_{f2}. Also, the bichromatic millimeter wave R_{xx} response varies nonlinearly with P, see Fig. 3, similarly to the non-linear variation observed in the monochromatic photoexcitation-induced magnetoresistance oscillations.[15] To understand these observations, we first provide a displacement theory-inspired picture to help understand the B-response under bichromatic excitation.[1,37,38,40,42,43,48] Following this qualitative description, numerical simulation results of the diagonal resistance is presented using the radiation-driven electron orbit model.[38,48]

A. Qualitative displacement-type explanation

A transverse B-field applied to a parabolic 2DES system produces Landau levels with energy spacing given by $E = \hbar\omega_c(B)$. In the swept-B, constant-f experiment, the energy separation between Landau levels increases with the increment of B while the millimeter wave photon energies, $E = hf$, remain constant, see Fig. 5. The constant photon energies are shown as green and red arrows in Fig. 5 for the bichromatic experiment, for the low- and high- frequency millimeter wave f components, respectively.

To explain the experimental observations, we reason that lower frequency, i.e., photoexcitation that spans fewer Landau levels, provides a greater contribution to the magnetoresistive response than higher frequency photoexcitation. One might expect this feature if the photoexcited transition probability associated with crossing fewer Landau levels at the lower frequency is greater than it is for crossing more Landau levels at the higher frequency. Then, the time interval for the excitation to the higher Landau level is shorter at the lower frequency than the higher frequency. With bichromatic excitation, the lower frequency will then induce the transition from the

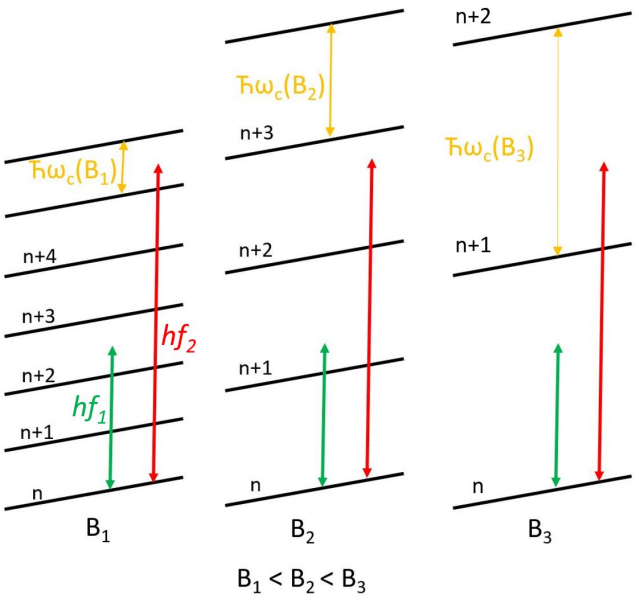

FIG. 5. Landau levels at magnetic fields that satisfy the relation $B_1 < B_2 < B_3$. The Landau levels are tilted by the electric field within the 2DES. The green and the red arrows illustrate inter Landau level transitions for the the low frequency- and high frequency millimeter waves, respectively. The figure conveys the point that low frequency photons span fewer Landau levels than the high frequency photons. Thus, associated transitions are of "lower order" at the lower frequency.

lower Landau level for a given carrier before the higher frequency radiation is able to do the same. As a result, for bichromatic photo-excitation, the lower frequency excitation will provide the stronger contribution to the diagonal resistance. Thus, for the specific case illustrated in Fig. 5, the order of excitation for high and low frequencies are about 5 and 2, respectively, at the magnetic field B_1. If the low order excitations tend to provide the greater contribution to R_{xx}, then the bichromatic diagonal resistance oscillation should follow the low frequency monochromatic response, which is what is observed at "low-B", as can be seen in Figs. 1 and 2. With the increase of the magnetic field, the Landau level separation progressively increases, and the picture shifts towards the illustration for B_2 in Fig. 5. Now, since the order of excitation for high and low frequencies are close to 3 and 1, respectively, the lower millimeter wave frequency in the bichromatic experiment should still dominate. But since the order of excitation of the higher frequency component is not as high as at B_1 it should also contribute more than in previous case, so we should observe a deviation in the bichromatic response from the low frequency response towards the high frequency response, which can be observed in the experimental results. Finally, when the magnetic field is further increased to B_3, the Landau level separation increases even more such that the low frequency excitation-order becomes less than 1, as the high frequency excitation-order approaches 1. In this case, the bichromatic R_{xx} response ought to shift towards the high frequency response for R_{xx}, which is also observed in experiment. This qualitative reasoning serves only to provide some intuitive understanding as to how deviations in the magnetoresistive response from *simple superposition with equal weight to the two frequency components* can come about.

B. Modeling based on the radiation-driven electron orbit theory

A semiclassical approach to explain the experimental results can be obtained by using the radiation-driven electron orbit theory[38]. This model was proposed to study the striking effects of radiation-induced resistance oscillations and zero resistance states. According to this model, when a Hall bar is illuminated, the guiding centers of the Landau states (LS) perform a classical trajectory consisting in a harmonic motion along the direction of the current. Thus, the electron orbits move in phase and harmonically with each other at the radiation frequency, altering dramatically the scattering conditions and giving rise eventually to millimeter wave radiation-induced magnetoresistance oscillations and, at higher P, the zero-resistance states.[1] The key parameter is the average advanced distance by the scattered electron between LS, given by[64] $\Delta X(t) = \Delta X_0 - A\sin\left(2\pi\frac{w}{w_c}\right)$ where A is the amplitude of the radiation driven orbit motion, $A = \frac{eE_o}{m^*\sqrt{(w_c^2-w^2)^2+\gamma^4}}$, and $w = 2\pi f$, with f the radiation frequency. In the expression of A, E_0 is the radiation electric field and γ is a phenomenologically-introduced damping factor for the interaction of electrons with the lattice ions giving rise to the emission of acoustic phonons. ΔX^0 is the average advanced distance by the electron due to scattering between Landau orbits without radiation. Then applying the Boltzmann transport theory we finally obtain the longitudinal magnetoresistance, $R_{xx} \propto \int dE \frac{(\Delta X(t))^2}{\tau_q}$ for energy E, where $\frac{1}{\tau_q}$ is the remote charged impurity scattering rate.

When we irradiated the 2DES with two sources of different frequency, $w_1 = 2\pi f_1$ and $w_2 = 2\pi f_2$, the Landau orbit guiding center is driven simultaneously by two different time-dependent sinusoidal forces with amplitudes A_1 and A_2, giving rise to interference effects. Now the average advanced distance is $\Delta X_1(t) + \Delta X_2(t)$, and the longitudinal magnetoresistance,[65] $R_{xx} \propto \int dE \frac{[\Delta X_1(t)+\Delta X_1(t)]^2}{\tau_q}$. According to the last expression we will obtain different responses depending on the relative values of frequency, phase difference and intensity of the radiations fields.

In Fig. 6 we plot simulations of irradiated R_{xx} vs. B for the same radiation parameters as in Fig. 1. We obtain calculated results in reasonable agreement and with the same trends as in experiments. However, some small differences can be observed. For instance, in the mini-

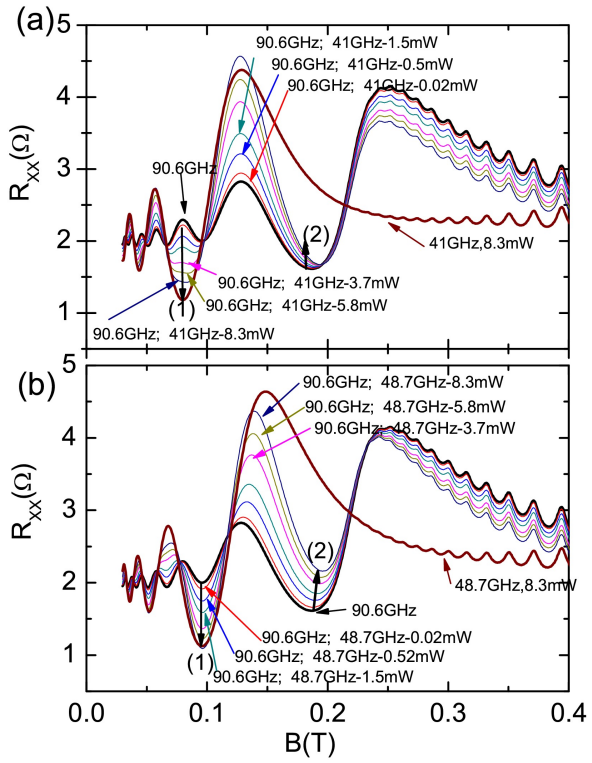

FIG. 6. Calculated irradiated R_{xx} versus B, for the same radiation parameters as in Fig.1. The simulations are according to the radiation-driven electron orbit model. The results are in reasonable agreement with experiments except for the main minimum position labeled as (2).

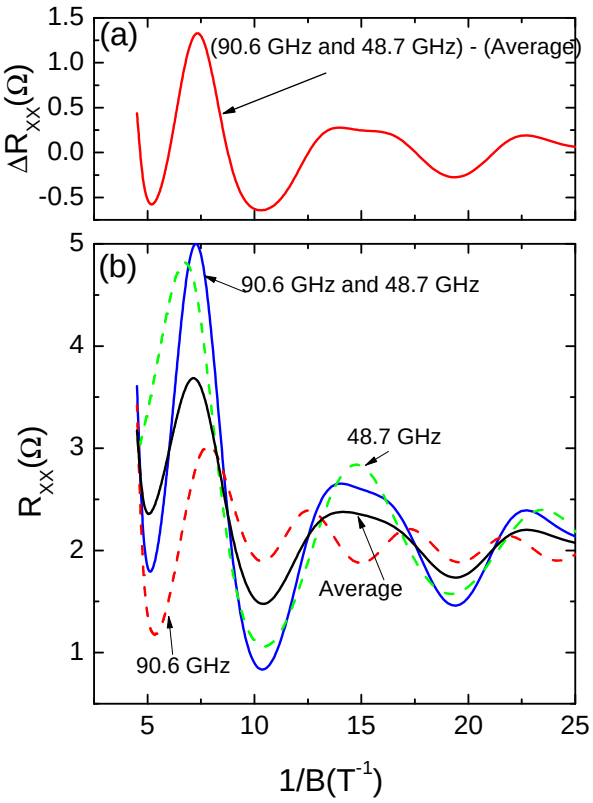

FIG. 7. Calculated irradiated resistances versus $1/B$. The simulations are obtained using the radiation-driven electron orbit model.[38] (a) The difference between the bichromatic (blue trace, panel (b), below) and average responses (black trace, panel (b), below). (b) R_{xx} vs. B^{-1} for monochromatic excitation at 90.6 GHz (dashed red), 48.7 GHz (dashed lime green), bichromatic excitation at 90.6 GHz and 48.7 GHz,(blue) and the numerical arithmetic average of the monochromatic signals at 90.6 GHz and 48.7 GHz(black).

mum labeled with (2), the theory obtains a shift to the right for increasing radiation power. Figure 7 shows the theoretical simulation results vs. $1/B$, in the same style as figure 4 shows the experimental results vs. $1/B$. Thus, this figure (Fig. 7 (b)) shows the modeling for the components as well as the full R_{xx}. Further, panel (a) of Fig. 7 shows ΔR_{xx} vs. $1/B$, where ΔR_{xx} is the difference between the theoretical bichromatic and average responses. This Fig. 7(a) may be compared with Fig. 4(a) which shows the experimental ΔR_{xx} vs. $1/B$. A comparision of Fig. 4(a) and Fig. 7(a) suggests that the theory captures the experimental observations.

According to this model the experimental results are mainly due to the damping effect of the denominator of A_1 and A_2 when B keeps increasing, especially beyond the resonance condition $w_c = w$. If $w_2 < w_1$, the damping takes place for the low frequency component (w_2) when B is high. Meanwhile, the high component still is important, becoming preponderant and setting R_{xx} for higher B. On the other hand, for lower B, it turns out that $A_2 >> A_1$, and for increasing intensity of the low frequency component becomes preponderant, eventually determining R_{xx}. Another consequence of this explanation is that the further apart the two radiation frequencies, the more important will be the predominance of the low frequency component at low B and of the high frequency component at high B.

IV. CONCLUSIONS

It appears that the millimeter wave-induced oscillatory magnetoresistance response under bichromatic excitation is not a simple, equally-weighted, arithmetic average of the two individual monochromatic magnetoresistive responses at f_1 and f_2. These results suggest that the bichromatic R_{xx} response tends to follow the monochromatic low frequency R_{xx} response at lower B, and it deviates towards the monochromatic high frequency R_{xx}

response with increasing the magnetic field strength at modest power levels for the two frequency components. This feature is qualitatively attributed here to the relative "order of excitations" for the two components. It was also observed that the extrema of the oscillatory diagonal resistance, R_{xx} for bichromatic excitation vary non linearly with the millimeter wave power, similar to the situation for monochromatic photo-excitation. Both these attributes may also be observed in numerical simulations of the diagonal resistance obtained using the radiation-driven electron orbit theory.[38]

V. ACKNOWLEDGEMENTS

BG, RLS, and magnetotransport studies at Georgia State University have been funded by U.S. Department of Energy, Office of Basic Energy Sciences, Material Sciences and Engineering division under the grant DE-SC0001762. HCL, microwave/millimeter/terahertz study, and 2D material study have been funded by Army Research Office under W911NF-14-2-0076 and W911NF-15-1-0433. JI is supported by the MINECO (Spain) under grant MAT2014-58241-P and ITN Grant 234970 (EU). Grupo de Matematicas Aplicadas a la Materia Condensada, (UC3M), Unidad Asociada al CSIC.

* rmani@gsu.edu

[1] R. G. Mani, J. H. Smet, K. von Klitzing, V. Narayanamurti, W. B. Johnson, and V. Umansky, Nature (London) **420**, 646 (2002).

[2] M. A. Zudov, R. R. Du, L. N. Pfeiffer, and K. W. West, Phys. Rev. Lett. **90**, 046807 (2003).

[3] R. G. Mani, V. Narayanamurti, K. von Klitzing, J. H. Smet, W. B. Johnson, and V. Umansky, Phys. Rev. B **70**, 155310 (2004); Phys. Rev. B. **69**, 161306 (2004).

[4] R. G. Mani, J. H. Smet, K. von Klitzing, V. Narayanamurti, W. B. Johnson, and V. Umansky, Phys. Rev. Lett. **92**, 146801 (2004); Phys. Rev. B **69**, 193304 (2004).

[5] A. E. Kovalev, S. A. Zvyagin, C. R. Bowers, J. L. Reno, and J. A. Simmons, Solid State Commun. **130**, 379 (2004).

[6] M. A. Zudov, R. R. Du, L. N. Pfeiffer, and K. W. West, Phys. Rev. Lett. **96**,236804 (2006).

[7] B. Simovic, C. Ellenberger, K. Ensslin, H. P. Tranitz, and W. Wegscheider, Phys. Rev. B **71**, 233303 (2005).

[8] R. G. Mani, Physica E **22**, 1 (2004); Physica E **25**, 189 (2004); Phys. Rev. B **72**, 075327 (2005); Appl. Phys. Lett. **91**, 132103 (2007); Physica E **40**, 1178 (2008); Appl. Phys. Lett. **92** 102107 (2008).

[9] J. H. Smet, B. Gorshunov, C. Jiang, L. Pfeiffer, K. West, V. Umansky, M. Dressel, R. Meisels, F. Kuchar, and K. von Klitzing, Phys. Rev. Lett. **95**, 116804 (2005).

[10] S. Wiedmann, G. M. Gusev, O. E. Raichev, T. E. Lamas, A. K. Bakarov, and J. C. Portal, Phys. Rev. B.**78**, 121301 (2008).

[11] D. Konstantinov and K. Kono, Phys. Rev. Lett. **103**, 266808 (2009).

[12] R. G. Mani, W. B. Johnson, V. Umansky, V. Narayanmurti, and K. Ploog, Phys. Rev. B**79**, 205320 (2009).

[13] O. M. Fedorych, M. Potemski, S. A. Studentikin, J. A. Gupta, Z. R. Wasilewski, I. Dmitriev, Phys. Rev. B **81**, 201302 (2010).

[14] Y. Dai, R. R. Du, L. N. Pfeiffer, and K. W. West, Phys. Rev. Lett. **105**, 246802 (2010).

[15] R. G. Mani, C. Gerl, S. Schmult, W. Wegscheider, and V. Umansky, Phys. Rev. B **81**, 125320 (2010).

[16] S. Wiedmann, G. M. Gusev, O. E. Raichev, A. K. Bakarov, and J. C. Portal, Phys. Rev. B**16**, 165303 (2011).

[17] A. N. Ramanayaka, R. G. Mani, and W. Wegscheider, Phys. Rev. B **83**, 165303 (2011).

[18] Y. H. Dai, K. Stone, I. Knez, C. Zhang, R. R. Du, C. L. Yang, L. N. Pfeiffer, and K. W. West, Phys. Rev. B **84**, 241303 (2011).

[19] R. G. Mani, A. N. Ramanayaka, and W. Wegscheider, Phys. Rev. B **84**, 085308 (2011); A. N. Ramanayaka, R. G. Mani, J. Inarrea, and W. Wegscheider, ibid. **85**, 205315 (2012).

[20] R. G. Mani, J. Hankinson, C. Berger, and W.A. de Heer, Nat. Commun. **3**, 996 (2012).

[21] R. G. Mani, A. N. Ramanayaka, T. Ye, M. S. Heimbeck, H. O. Everitt, and W. Wegscheider, Phys. Rev. B **87**,245308 (2013).

[22] T. Ye, R. G. Mani, and W. Wegscheider, Appl. Phys. Lett. **102**, 242113 (2013); **103**, 192106 (2013).

[23] R. G. Mani and A. Kriisa, Sci. Rep. **3**, 3478 (2013).

[24] R. G. Mani, A. Kriisa, and W. Wegscheider, Sci. Rep. **3**, 2747 (2013).

[25] T. Ye, H-C.Liu, W. Wegscheider,and R. G. Mani, Phys. Rev. B **89**, 155307 (2014).

[26] T. Ye, W. Wegscheider and R. G. Mani, Appl. Phys. Lett. **105**, 191609 (2014).

[27] H- C. Liu, T. Ye, W. Wegscheider and R. G. Mani, J. Appl. Phys. **117**, 064306 (2015).

[28] T. Ye, H.C. Liu, Z. Wang, W. Wegscheider and R. G. Mani, Sci. Rep. **5**, 14880 (2015).

[29] Z. D. Kvon et al., JETP Lett. 97, 41 (2013).

[30] A. D. Chepelianskii, J. Laidet, I. Farrer, D. A. Ritchie, K. Kono, and H. Bouchiat, Phys. Rev. B 90, 045301 (2014).

[31] S. Chakraborty, A. T. Hatke, L. W. Engel, J. D. Watson, and M. J. Manfra, Phys. Rev. B. **90**, 195437 (2015).

[32] A. D. Levin, Z. S. Momtaz, G. M. Guzev, O. E. Raichev, and A. K. Bakarov, Phys. Rev. Lett. **115** 206801 (2015).

[33] A. D. Chepelianskii, M. Watanabe, K. Nasyedkin, K. Kono, and D. Konstantinov, Nat. Comm. **6**, 7210 (2015).

[34] R. G. Mani, Appl. Phys. Lett. **108**, 033507 (2016); Z. Phys. B 92, 335 (1993).

[35] T. Ye, J. Inarrea, W. Wegscheider, and R. G. Mani, Phys. Rev. B **94**, 035305 (2016)

[36] J. Iñarrea, R. G. Mani, and W. Wegscheider, Phys. Rev. B **82**, 205321 (2010).

[37] A. C. Durst, S.Sachdev, N. Read, and S. M. Girvin, PhysRevLett. **91**, 086803 (2003).

[38] J. Iñarrea and G. Platero, Phys. Rev. Lett. **94**, 016806 (2005).

[39] A. V. Andreev, I. L. Aleiner, and A. J. Millis, Phys. Rev. Lett. **91**, 056803 (2003).

[40] V. Ryzhii and R. Suris, J.Phys.Condens.Matter **15**, 6855 (2003).
[41] A. A. Koulakov and M. E. Raikh, Phys. Rev.B **68**, 115324 (2003).
[42] V. Ryzhii, Phys. Rev. B **68**, 193402 (2003).
[43] X. L. Lei and S. Y. Liu, Phys. Rev. Lett. **91**, 226805 (2003).
[44] S. A. Mikhailov, Phys. Rev. B 70, 165311 (2004).
[45] I. A. Dmitriev, M. G. Vavilov, I. L. Aleiner, A. D. Mirlin, and D. G. Polyakov, Phys. Rev. B **71**, 115316 (2005).
[46] X. L. Lei and S. Y. Liu, Phys. Rev. B **72**,075345 (2005).
[47] X. L. Lei and S. Y. Liu , Appl. Phys. Lett. **89**, 182117 (2006).
[48] J. Iñarrea and G. Platero, Phys. Rev. B **76**, 073311 (2011).
[49] A. D. Chepelianskii and A. S. Pikovsky, and D. L. Shepelyansky, Eur. Phys. J. B**60**, 225 (2007).
[50] X. L. Lei, Physica E **42**, 63-66 (2009).
[51] A. D. Chepelianskii and D. L. Shepelyansky, Phys. Rev. B**80**, 241308 (2009).
[52] M. Khodas et al., Phys. Rev. Lett. 104, 206801 (2010).
[53] S. A. Mikhailov, Phys. Rev. B**83**, 155303 (2011).
[54] J. Iñarrea, Appl. Phys. Lett. **99**, 232115 (2011).
[55] X. L. Lei and S. Y. Liu, Phys. Rev. B**86**, 205303 (2012).
[56] J. Iñarrea, J. Appl. Phys. **113**, 183717 (2013).
[57] A. Kunold and M. Torres, Physica B**425**, 78 (2013).
[58] O. V. Zhirov, A. D. Chepelianskii, and D. L. Shepelyansky, Phys. Rev. B**88**, 035410 (2013).
[59] X. L. Lei and S. Y. Liu, J. Appl. Phys. **115**, 233711 (2014).
[60] A. Yar and K. Sabeeh, J. Phys.:Cond. Matt. **27**, 435007 (2015).
[61] V. G. Ibarra-Sierra, J. C. Sandoval-Santana, J. L. Cardoso, and A. Kunold, Annal. Phys. **362**, 83 (2015).
[62] O. E. Raichev, Phys. Rev. B **91**, 235307 (2015).
[63] Y. M. Beltukov and M. I. Dyakonov, Phys. Rev. Lett. **116**, 176801 (2016).
[64] Jesus Inarrea, Euro. Phys Lett., **113**, 57004, (2016).
[65] J. Inarrea and G. Platero, Appl. Phys. Lett. **89**, 172114, (2006).